Mitigation of energetic ion debris from Gd plasma using dual laser pulses and the combined effect with ambient gas*

Dou Yin-Ping(窦银萍), Sun Chang-Kai(孙长凯)†, Liu Chao-Zhi(刘超智), Gao Jian(高 健), Hao Zuo-Qiang(郝作强), and Lin Jing-Quan(林景全)‡

School of Science, Changchun University of Science and Technology, Changchun 130022, *China*

(Received 21 October 2013; revised manuscript received 2 January 2014; published online 15 May 2014)

For the next-generation beyond extreme ultraviolet lithography (EUVL) sources, gadolinium (Gd) plasma with emission wavelength at 6.7 nm seems to be the leading candidate. Similar to the Sn target 13.5 nm light source, ion debris mitigation is one of the most important tasks in the laser-produced Gd plasma EUV source development. In this paper, a dual-laser-pulse scheme, which uses a low energy pulse to produce a pre-plasma and a main pulse after a time delay to shoot the pre-plasma, is employed to mitigate the energetic ion generation from the source. Optimal conditions (such as pre-pulse energy and wavelength, and the time delay between the pre-pulse and the main pulse for mitigating the ion energy) are experimentally obtained, and with the optimal conditions, the peak of the ion energy is found to be reduced to 1/18 of that of a single laser pulse case. Moreover, the combined effect by applying ambient gas to the dual-pulse scheme for ion debris mitigation is demonstrated, and the result shows that the yield of Gd ions is further reduced to around 1/9 of the value for the case with dual laser pulses.

Keywords: extreme ultraviolet source, laser-induced plasma, Gd plasma, ion debris

PACS: 52.38.–r, 52.59.Px, 52.59.Ye **DOI:** 10.1088/1674-1056/23/7/075202

1. Introduction

Extreme ultraviolet lithography (EUVL) at 13.5 nm for high-volume manufacturing (HVM) of integrated circuits (ICs) with node sizes of 32 nm or less has nearly reached the stage of industrial production.[1,2] In order to further shrink the node size, the development of EUV sources of emission with wavelengths less than 10 nm is a subject of considerable interest.[3] Recently, a laser produced plasma (LPP) EUV source[4–6] operating in the 6.x nm region based on rare-earth targets of Gd and Tb has been demonstrated,[7] and its peak emission wavelength matches the operating wavelength of the Mo/B_4C multilayer reflective mirror, so it could be used as the light source for future lithography, the so-called beyond EUVL. Generally, the emitting ions in Gd plasmas have an electronic structure similar to that of Sn,[8] where the in-band radiation is from 4d–4f, 4p–4d, and 4d–5p transitions of Gd from charge state Gd^{17+} to charge state Gd^{25+}. Unavoidably, the source emits a large amount of ion debris resulting from the interaction of high intensity laser pulse with plasma. Therefore, the LPP Gd plasma source will cause a serious energetic ion pollution, the same as the Sn target light source. Moreover, this may be even worse for the Gd target 6.7 nm source in terms of energetic ion debris, as the simulation results on laser and plasma parameters for the optimized in-band EUV conversion efficiency show that much higher laser intensity, plasma temperature, and ionization stage are required for the 6.7 nm light source compared with the 13.5 nm source.[9] Therefore, the mitigation of ion debris from the laser plasma Gd target source remains a key issue to be solved, and indeed it is an arduous task for the source developers.

So far, various methods have been applied to control the debris of an LPP source, including mass limited droplet target, tape target, applying external magnetic fields or ambient gas, dual-laser-pulse technology, and so on.[10–14] Among those methods, the dual-pulse technology is a very promising candidate for effectively mitigating energetic ions from the plasma. In a laser plasma, the ion acceleration is mainly due to the electrostatic field created by the freed electrons, and the maximum electric field is expressed as $E_{\max} = k_B T_e / e l_{ss}$, where T_e is the electron temperature, e is the elementary charge, and l_{ss} is the initial scale length of the ion density.[15] Therefore, an important parameter that affects the efficiency of the ion acceleration is the initial scale length at the plasma surface. The dual-pulse technology employs the main laser pulse to heat up a pre-plasma of smooth ion density,[16] which gives a longer initial scale length l_{ss} compared to the case of single pulse, and correspondingly a smaller maximum electrostatic field $E_{\max}$. Therefore, the smooth ion density of the double-pulse scheme results in a reduction of the maximum ion ve-

*Project supported by the National Basic Research Program of China (Grant No. 2013CB922404), the National Natural Science Foundation of China (Grant Nos. 11074027, 61178022, 11274053, and 11211120156), the Science & Technology Department of Jilin Province, China (Grant No. 20111812), the Research Fund for the Doctoral Program of Higher Education of China (Grant Nos. 20122216120009, 20122216110007, and 20112216120006), and the Young Scientists Fund of Changchun University of Science and Technology, China (Grant No. 000520).

†Corresponding author. E-mail: changkaisun@cust.edu.cn

‡Corresponding author. E-mail: linjingquan@cust.edu.cn

© 2014 Chinese Physical Society and IOP Publishing Ltd

locity. Experimentally, it has been proven that the double-pulse scheme is a powerful method to mitigate the energetic ions.[16–18] The double-pulse scheme can effectively stop the energetic ion from reaching the EUV multilayer collector, it could also benefit the EUV conversion efficiency enhancement in the EUV light source through plasma control. Compared to the case of a single laser pulse, previous research on the 13.5 nm EUV source with dual laser pulses has shown that the conversion efficiency of the in-band EUV emission at 13.5 nm was enhanced to 1.25-fold for an Sn solid target with an optimal delay time of around 400 ns for pre- and main-pulses, and enhanced to 3.4-fold for an SnO_2 nanoparticle target with a delay time of around 150 ns.[18,19]

In addition to the mitigation of ion debris by using the dual-laser-pulse scheme, some ambient gas (such as argon or helium) can effectively stop the energetic Sn ions at a low operating pressure and meanwhile provide exceptionally good transmission to the EUV radiation.

In this paper, we report an investigation of the energetic ion mitigation with the dual-pulse scheme and the combined effect with ambient gas. The dependence of the Gd ion energy on pre-pulse wavelength, energy, delay between pre-pulse and main pulse, and the angular dependence of the mitigation effect of the dual-pulse technology are studied. Furthermore, the effect of the synergistic reaction to mitigate Gd ions by combining the dual pulses with ambient gas is demonstrated. To the best of our knowledge, an investigation of the energetic ion mitigation for the emerging beyond EUVL source at 6.7 nm with a Gd target has not been reported before.

2. Experiment

The experimental setup for characterizing and mitigating debris is shown in Fig. 1. The Gd target with a thickness of 2 mm is fixed on a three-dimensional motorized translation stage in a vacuum chamber, and the chamber can be pumped down to $\sim 10^{-5}$ Torr by a turbo pump and a pre-stage pump. Two YAG lasers are employed for the dualpulse generation in our experiment. One is a Nd:YAG laser (Innolas Splitlight Compact 400), which can deliver laser at the wavelengths of 1064 nm, 532 nm, and 355 nm and with pulse durations of ~8 ns. This laser is used to generate the pre-plasma. The other laser is a *Q*-switched Nd:YAG laser (Continuum, Powerlite Precision II) operating at 1064 nm which delivers pulses with maximum energy of 1 J and duration of 10 ns. This laser is used to generate the main pulses to heat the pre-plasma for mitigating the energetic ions. The main laser intensity used in the experiment is about 7×10^{11} W/cm^2, which is close to the optimum intensity for the highest conversion efficiency at 6.7 nm.[20] The delay time between the pre-pulse and the main laser pulse is controlled with a pulse generator (Stanford Research, DG 645). To measure ion signals from the Gd plasma, a set of four Faraday cups are used as the ion detectors, which are placed at a distance of 15 cm away from the Gd plasma and arranged at angles of 18°, 36°, 54°, and 72° related to the target normal respectively. The time-of-flight (TOF) method is used to measure the kinetic energy of the ions. The ion signal obtained with the Farady cups is displayed by a 2.5-GHz digital oscilloscope. Ar and He are used as the ambient gases to mitigate the ion debris.

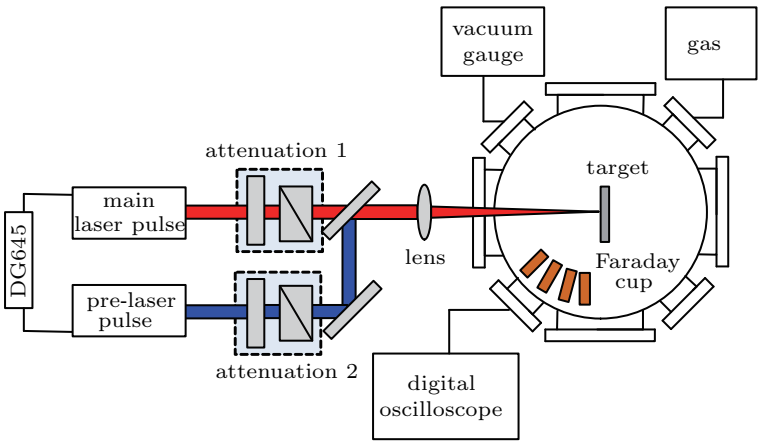


Fig. 1. (color online) Experiment setup of the system with ion debris mitigation by dual pulses.

3. Results and discussion

A typical TOF ion signal recorded from the Gd target plasma with a single laser pulse is given in Fig. 2. The Nd:YAG laser pulse intensity is 7×10^{11} W/cm^2, and the wavelength of the laser is 1064 nm. As shown in Fig. 2, there is a twin-peak structure in the TOF signal for the Gd target plasma. The faster and sharper peak close to time zero is the fast electron signal and results from the photo-electric effect,[21] and the first peak is defined as a zero-time marker. The broad and intense signal after the fast electron signal is from the Gd ions, and it shows a flux peak of thermal Gd ions arriving at the Farady cup with a TOF of 2.1 μs, corresponding to an ion energy of 3.7 keV.

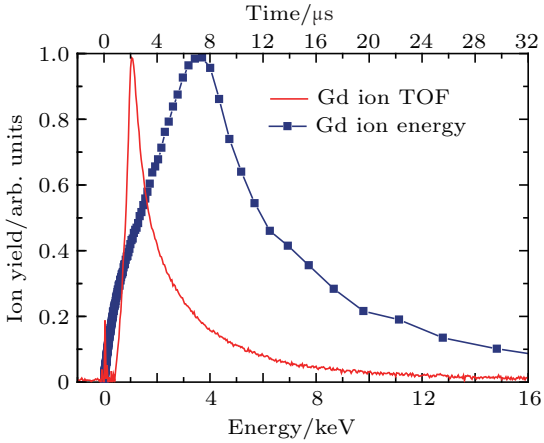


Fig. 2. (color online) A typical TOF ion signal from the Gd target plasma and the corresponding ion energy using the single laser pulse at a detecting angle of 18° with respect to the target normal.

The effect of the pre-pulse laser energy on the ion kinetic energy is investigated. Figure 3 shows the ion energy distributions from laser-produced Gd plasmas in the dual-pulse scheme. The main laser wavelength is 1064 nm, the delay time between the pre-pulse and the main laser pulse is fixed at 100 ns, and the pre-pulse laser energy increases from 0.6 mJ to 50 mJ at the wavelength of 355 nm. For comparison, the ion energy distribution with the single laser pulse is also given in the figure. It is seen that the kinetic energies of the ion debris coming from the single pulse and the dual pulses can be described by a shifted Maxwell–Boltzmann distribution. The peak of the thermal ion energy is about 3.7 keV with the single laser pulse. When the pre-pulse is used, the shape of the ion energy distribution is different from that of the single laser pulse, and the ions with high energy are greatly mitigated and all ions are shifted towards low energy. The introduction of the pre-pulse makes the main laser pulse heat up a pre-plasma of smooth ion density instead of interacting with a sharp density profile plasma resulting from the laser interaction with the solid density target surface. Electron cooling and wave breaking in the process of plasma expansion with an initially smooth ion density may lead to producing slower ions contrast to that with a plasma having an initial sharp boundary profile.[22,23] It is shown that the peak of the ion energy shifts towards lower energy with the increase in the pre-pulse energy, and the peak of the ion energy is reduced to around 0.5 keV as the pre-pulse energy is increased to about 40 mJ. There is no further ion energy reduction when the pre-pulse laser energy is further increased to 50 mJ; however, a small intensity increase in the ions signal is found. The further increase in the ion signal intensity may be due to the fact that a much higher pre-pulse energy can cause the energetic ions' self generation.

The effect of the time delay between the pre-pulse and the main pulse on the ion debris energy distribution is investigated at pre-pulse energy of 40 mJ and wavelength of 1064 nm. The ion energy distributions driven by dual pulses with various time delays are shown in Fig. 4. The ions with high energy are obviously mitigated and the ion energy is shifted towards lower energy as the time delay increases. It is seen that the flux peak is largely reduced as the delay time is increased up to 400 ns, both the ion yield and the kinetic energy of most thermal ions resulting from the interaction between the laser pulse and the LPP decrease obviously with increasing time delay, until the time delay is 550 ns. The flux peak of the thermal ion energy will keep almost the same as the case of 550 ns delay when the time delay further increases. In addition, we note that the flux peak of the thermal ion energy with a large reduction in the delay time of 400–500 ns as observed in Fig. 4 is in agreement with the optimal delay time for maximizing the EUV conversion efficiency using the double-pulse scheme in the previous Sn target experiments.[18,19]

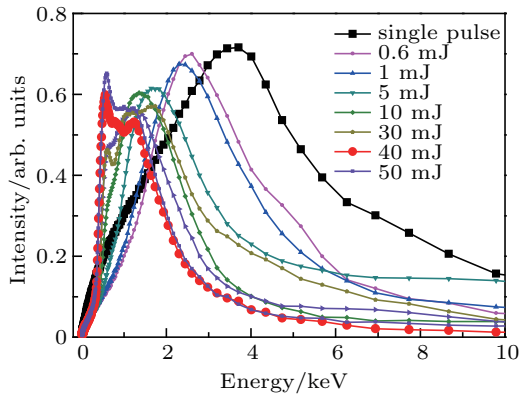


Fig. 3. Typical ion energy distributions from the Gd target driven with dual pulses with various pre-pulse laser energy at detecting angle of 18° with respect to the target normal. In order to clearly present the data we select the ion energy in the range of less than 10 keV in this figure.

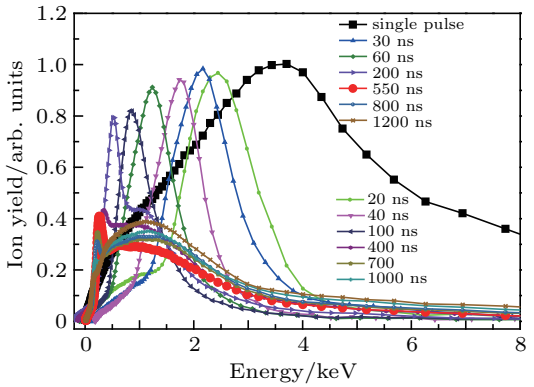


Fig. 4. (color online) Typical ion energy distributions from the Gd target driven with dual laser pulses with different time delays between the pre-pulse and the main laser pulse at the angle of 18° with respect to the target normal.

The effect of the wavelength of the pre-pulse on the energy of the ion debris is also investigated. The ion energy distributions at the detecting angle of 18° to the normal of the target irradiated by pre-pulse lasers of 1064 nm, 532 nm, and 355 nm, respectively, are shown in Fig. 5. The laser energy for generating pre-plasma and the time delay adopt the optimized

values, which are 40 mJ and 55 ns, respectively. It is noted that the peak of the ion energy corresponds to a minimum value of about 0.20 keV with 355 nm laser as the pre-pulse, which is about 1/18 of the energy of most thermal ions obtained with the single laser pulse. In the meantime, the ion yield is also the lowest with 355 nm pre-pulse laser.

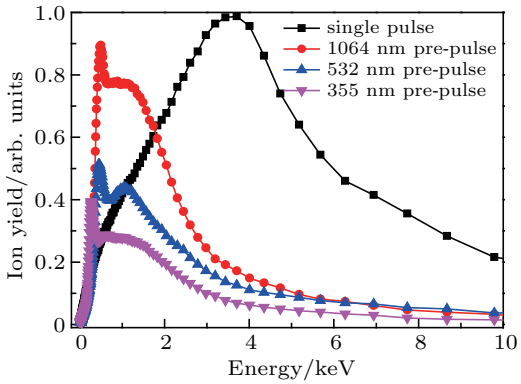


Fig. 5. (color online) The TOF ion signals from the Gd target irradiated with pre-pulse laser of different wavelengths at the angle of 18° with respect to the target normal.

The 355 nm pre-laser pulse gives the minimum ion energy, which can be explained as follows. The scaling law for mass-ablation rate $\dot{m}$ of a laser incident on a target is[24]

$$\dot{m} = 3 \times 10^3 I^{5/9} A^{3/8} \lambda^{-4/9},$$

where I is the laser intensity, λ is the wavelength of the laser, and A is the atomic number. If the same laser intensity is used in the experiment, the mass-ablation rate will vary with the excitation wavelength as $\lambda^{-4/9}$. Hence, the laser–target coupling efficiency is higher for a shorter wavelength, which generates a denser plasma. Meanwhile, the dominating absorption mechanism in the plasma is the inverse Bremsstrahlung, which is inversely proportional to the wavelength of the laser pulse. The Gd target absorbs more laser pulse energy when a shorter wavelength (355 nm) laser is used, generating a much larger scale plasma.[18] Therefore, the 1064 nm main laser pulse will be absorbed much more when it travels through the pre-plasma generated with the shorter wavelength laser, which helps to reduce the main laser pulse to ablate the solid target directly, resulting in a reduction of the energetic ion generation.

The angular dependence on the mitigation effect of the dual-pulse technology is also investigated. Figure 6 shows the angular distributions of the flux peaks of the Gd ions at 18°, 36°, 54°, and 72°, respectively, with respect to the target normal obtained by dual laser pulses under the optimized conditions and those by the single laser pulse. The results clearly show that the flux peak of the ion energy is largely decreased with the increase of the detecting angle in the single laser pulse case, and the ion energies at different collecting angles are all reduced to around 0.20 keV for the case with the dual laser pulses, which are independent of the detecting angle. This shows that this technique is effective in reducing the ion kinetic energy over a large range of detecting angles. Most importantly, the energy of the ions at small angles with respect to the target normal direction, where most intense EUV radiation is emitted from the source,[25] is greatly reduced in the double-laser-pulse scheme.

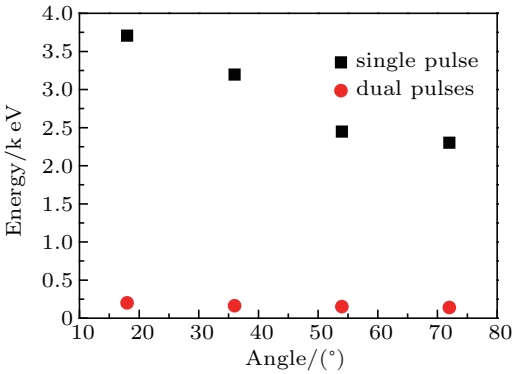


Fig. 6. (color online) The kinetic energy angular distributions of most Gd ions from TOF record at the angles of 18°, 36°, 54°, and 72° with respect to the target normal for the single laser pulse case and the dual-laser-pulse case with optimal conditions.

In the following, the combined mitigation effect of applying ambient gas to the dual-pulse scheme is presented. The results of synergistic reaction, which include cases of combining dual laser pulses with ambient gas and combining single laser pulse with ambient gas are shown in Fig. 7.

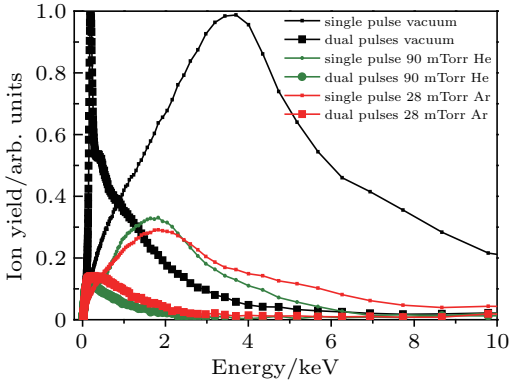


Fig. 7. (color online) The ion energy distributions under single and dual pulses combined with Ar and He as the ambient gas.

It is interesting to note that the amount of ion energy reduction by applying a low operation pressure ambient gas to the single pulse case is not as much as that of using double laser pulses without ambient gas. Meanwhile, it is noticeable that one obtains the best ion energy reduction effect for the case of the double laser pulses with ambient gas. As shown in Fig. 7, the peak of the ion energy is reduced to tens of eV when 90 mTorr He or 28 mTorr Ar is applied to the double-pulse case. The ion flux peak is much more effectively depressed for the case of the dual laser pulses than that of the

single laser pulse under the same ambient pressure condition. This suggests that the mitigation power of a neutral gas to the fast ions at the current pressure is not so strong as that to the slow ones. The difference in stopping power between the fast and the slow ions can be explained by the stopping nature of a gas. The stopping power S of a gas can be simply described as[26]

$$S = kZ_1Z_2^2L/\beta^2,$$

where $k = 0.3071/Z_2$, k is in units of keV/(mg/cm^2), Z_1 and Z_2 are the particle and the ambient gas atomic numbers, respectively, L is the stopping number, and $\beta = v/c$ is the relative velocity of the particles, with c being the velocity of light. As the stopping power is inversely proportional to the square of the ion velocity, the gas is more effectively to control the slow ions than the fast ones. The gas exhibits an excellent ability to mitigate the Gd ions in the case of the double laser pulses as observed in Fig. 7, thanks to the fact that the velocities of the Gd ions are already greatly reduced due to the interaction with the dual laser pulses. It is worth noting that the EUV light absorption by the ambient gas is quite small at current pressure, the calculation results show that transmissions of 99.2% for 28 mTorr Ar and 99.6% for 90 mTorr He are obtained for traveling a distance of 15 cm with the wavelength of 6.7 nm.[27]

4. Conclusion

We experimentally obtain the optimal conditions, including pre-pulse energy and wavelength, and the time delay between the pre-pulse and the main pulse, for mitigating the ion energy at the main laser intensity close to the optimum intensity for the highest conversion efficiency at 6.7 nm. It is found that the kinetic energy of the thermal ion debris peak under the optimized conditions can be reduced to 1/18 of that with a single pulse. A large reduction in the ion energy is due to the fact that the main laser pulse interacts with a lower and smoother pre-plasma instead of the initial solid density target. Moreover, adding ambient gas to the dual-pulse scheme enhances the ability in the mitigation of Gd ions resulting from the LPP source. The results on the Gd ion mitigation obtained in this work can provide basic understanding on the ion debris mitigation for a debris-free 6.7 nm beyond EUVL light source.

References

[1] Namba S, Fujioka S, Nishimura H, Yasuda Y, Nagai K, Miyanaga N, Izawa Y, Mima K and Takiyama K 2006 *Appl. Phys. Lett.* **88** 171503
[2] Morris O, Reilly F O, Dunne P and Hayden P 2008 *Appl. Phys. Lett.* **92** 231503
[3] Dou Y P, Sun C K and Lin J Q 2013 *Chin. Opt.* **6** 22 (in Chinese)
[4] Dong Q L, Zhang J, Wang S J, Zhao J and Li Y J 2007 *Chin. Phys.* **36** 609
[5] Zheng Z Y, Zhang Y, Wu X W, Lu X, Li Y T and Zhang J 2007 *Chin. Phys.* **36** 236
[6] Wang W, Zhang J and Senecha V K 2002 *Acta Phys. Sin.* **51** 590 (in Chinese)
[7] Otsuka T, Kibane D, Higashiguchi T, Yatagai N, Yatagai T, Jiang W H, Endo A, Dunne P and O'Sullivan G 2010 *Appl. Phys. Lett.* **97** 231503
[8] Otsuka T, Kilbane D, White J, Higashiguchi T, Yugami N, Yatagai T, Jiang W H, Endo A, Dunne P and O'Sullivan G 2010 *Appl. Phys. Lett.* **97** 111503
[9] Cummins T, Otsuka T, Yugami N, Wei H J, Endo A, Li B W, O'Gorman C, Dunne P, Sokell E, O'Sullivan G and Higashiguchi T 2012 *Appl. Phys. Lett.* **100** 061118
[10] Shinsuke F, Masashi S, Yoshinori S, Shinsuke M, Hirokazu S, Yuki N, Tatsuya A, Hiroaki N, Norimasa O, Atsushi S, Katsunobu N, Noriaki M, Yasukazu I and Kunioki M 2008 *Appl. Phys. Lett.* **92** 241502
[11] Haney S J, Berger K W, Kubiak G D, Rockett P D and Hunter J 1993 *Appl. Opt.* **32** 6934
[12] Harilal S S, O'Shay B and Tillack M S 2005 *J. Appl. Phys.* **98** 036102
[13] Azuma H, Nishimura Y, Sakata A and Takeuchi A 2002 *Appl. Surf. Sci.* **197** 224
[14] Dunne P, O'Sullivan G and O'Reilly D 1999 *Appl. Phys. Lett.* **76** 34
[15] Grismayer T and Mora P 2006 *Phys. Plasmas* **13** 032103
[16] Tao Y, Tillack M S, Harillal S S, Sequoia K L and Najmabadi F 2007 *J. Appl. Phys.* **101** 023305
[17] Tao Y and Tillack M S 2006 *Appl. Phys. Lett.* **89** 111502
[18] Freeman J R, Harilal S S and Hassanein A 2011 *J. Appl. Phys.* **110** 083303
[19] Higashiguchi T, Dojyo N, Hamada M, Sasaki W and Kubodera S 2006 *Appl. Phys. Lett.* **88** 201503
[20] Otsuka T, Kilbane D, White J, Higashiguchi T,Yugami N, Yatagai T, Jiang W H, Endo A, Dunne P and O'Sullivan G 2010 *Appl. Phys. Lett.* **97** 111503
[21] Sun Y B, Lin J Q, Gao X and Zhao Z M 2012 *Sci. Chin. Phys. Mech. Astron.* **55** 392
[22] Mora P 2005 *Phys. Plasmas* **12** 112102
[23] Grismayer T and Mora P 2006 *Phys. Plasmas* **13** 032103
[24] Burdt R A, Yuspeh S, Sequoia K L, Tao Y Z, Tillack M S and Najmabadi F 2009 *J. Appl. Phys.* **106** 033310
[25] Morris O, OReilly F, Dunne P and Hayden P 2008 *Appl. Phys. Lett.* **92** 231503
[26] Ziegler J F 1999 *J. Appl. Phys.* **85** 1249
[27] http://henke.lbl.gov/optical_constants/gastrn.html